Published OnlineFirst June 2, 2009; DOI: 10.1158/0008-5472.CAN-09-0354

Cancer Research

Extracellular Engagement of α₆ Integrin Inhibited Urokinase-Type Plasminogen Activator –Mediated Cleavage and Delayed Human Prostate Bone Metastasis

Michael O. Ports, Ray B. Nagle, Gerald D. Pond, et al.

Cancer Res Published OnlineFirst June 2, 2009.

Published OnlineFirst June 2, 2009; DOI: 10.1158/0008-5472.CAN-09-0354
Published Online First on June 2, 2009 as 10.1158/0008-5472.CAN-09-0354

Research Article

Extracellular Engagement of α_6 Integrin Inhibited Urokinase-Type Plasminogen Activator–Mediated Cleavage and Delayed Human Prostate Bone Metastasis

Michael O. Ports,[1] Ray B. Nagle,[1,2] Gerald D. Pond,[3] and Anne E. Cress[1,4]

[1]Cancer Biology Interdisciplinary Graduate Program and Departments of [2]Pathology, [3]Radiology, and [4]Cell Biology and Anatomy, University of Arizona, The Arizona Cancer Center, Tucson, Arizona

Abstract

Expression of α_6 integrin, a laminin receptor, on tumor cell surfaces is associated with reduced patient survival and increased metastasis in a variety of tumors. In prostate cancer, tumor extracapsular escape occurs in part via laminin-coated nerves and vascular dissemination, resulting in clinically significant bone metastases. We previously identified a novel form of α_6 integrin, called α_6p, generated by urokinase-type plasminogen activator-dependent cleavage of the laminin-binding domain from the tumor cell surface. Cleavage increased laminin-dependent migration. Currently, we used the known conformation sensitivity of integrin function to determine if engagement of the extracellular domain inhibited integrin cleavage and the extravasation step of metastasis. We show that α_6 integrin was present on prostate carcinoma escaping the gland via nerves. Both endogenous and inducible levels of α_6p were inhibited by engaging the extracellular domain of α_6 with monoclonal antibody J8H. J8H inhibited tumor cell invasion through Matrigel. A severe combined immunodeficient mouse model of extravasation and bone metastasis produced detectable, progressive osteolytic lesions within 3 weeks of intracardiac injections. Injection of tumor cells, pretreated with J8H, delayed the appearance of metastases. Validation of the α_6 cleavage effect on extravasation was confirmed through a genetic approach using tumor cells transfected with uncleavable α_6 integrin. Uncleavable α_6 integrin significantly delayed the onset and progression of osseous metastases out to six weeks post-injection. The results suggest that α_6 integrin cleavage permits extravasation of human prostate cancer cells from circulation to bone and can be manipulated to prevent metastasis. [Cancer Res 2009;69(12):5007–14]

Introduction

The α_6 integrin, a laminin receptor, is expressed on tumor cell surfaces and is associated with poor patient prognosis, reduced survival, and increased metastasis in a variety of tumors (1–4). Integrins are type I transmembrane heterodimers composed of α and β subunits. The heterodimer confers ligand-binding specificity to a particular extracellular matrix substrate (5). Integrins $\alpha_6\beta_1$ or $\alpha_6\beta_4$ are receptors for laminin 111 (laminin 1), laminin 511 (laminin 10), or laminin 332 (laminin 5), respectively. In human prostate cancer, escape from the gland occurs in part via laminin 511-coated nerves (6, 7) followed by dissemination and subsequent escape from circulation, resulting in clinically significant bone metastasis (8, 9). Additionally, mouse and human bone marrow have both been shown to be rich laminin environments (10–12).

The two most persistently expressed integrin heterodimer pairs in human prostate cancer are the laminin-binding $\alpha_6\beta_1$ and $\alpha3\beta_1$ receptors (13–15). In addition, the basement membrane component laminin 332 is not expressed, whereas laminin 511 persists, creating an environment selective for $\alpha_6\beta_1$ function (16). We previously reported a novel form of α_6 integrin, called α_6p, generated by cleavage of the laminin-binding domain from the tumor cell surface by urokinase-type plasminogen activator (uPA), a prometastatic factor (17, 18). Expression levels of both uPA and its cognate receptor were shown to be negatively correlated with prostate cancer patient survival (19, 20). The uPA-dependent cleavage of α_6 integrin increased cellular migration *in vitro* and was proposed as a mechanism for tumor cell release from adhesion to laminin (21). We initiated the current study to determine whether inhibiting cleavage of the $\alpha_6\beta_1$ integrin would alter the ability of tumor cells to reach the bone from the circulation.

Integrins provide linkage from the extracellular environment to intracellular cytoskeletal components that focally interact at the internal portion of the receptor. This integrated function is necessary for cellular adhesion, migration, survival, and differentiation (13). Integrin function is dictated in part by changes in receptor conformation that results in the alteration of ligand affinity and "outside-in" signaling (22, 23). This was initially inferred by the generation of monoclonal antibodies that could bind extracellular domains and alter integrin conformation and activity. Experimentally, integrins can be activated or functionally blocked from adhesion by externally applied antibodies (24). Circulating levels of immunoglobulins that engage and block adhesion function of the $\alpha_6\beta_1$ heterodimer, in patients with oral pemphigoid, results in formation of blisters and erosive lesions in the oral mucosa (25, 26).

We reasoned that engagement of extracellular epitopes on the receptor with α_6 integrin antibodies would block uPA-mediated cleavage. We report here the activity of the previously characterized J8H antibody that does not affect cellular adhesion on laminin (27) but does block integrin cleavage. J8H was used to test the influence of blocking integrin cleavage on the appearance of bone metastasis. A separate genetic approach, tumor cells expressing an uncleavable α_6 integrin mutant (21, 28), was used as an independent technique to determine if extravasation required integrin cleavage.

Materials and Methods

Antibodies and reagents. J8H, a mouse monoclonal antibody, recognizes an extracellular epitope of α_6 integrin and was a generous gift from

Requests for reprints: Anne E. Cress, 1515 North Campbell Avenue, Tucson, AZ 85724-5044. Phone: 520-626-7553; Fax: 520-626-4979; E-mail: acress@azcc.arizona.edu.

doi:10.1158/0008-5472.CAN-09-0354

Published OnlineFirst June 2, 2009; DOI: 10.1158/0008-5472.CAN-09-0354

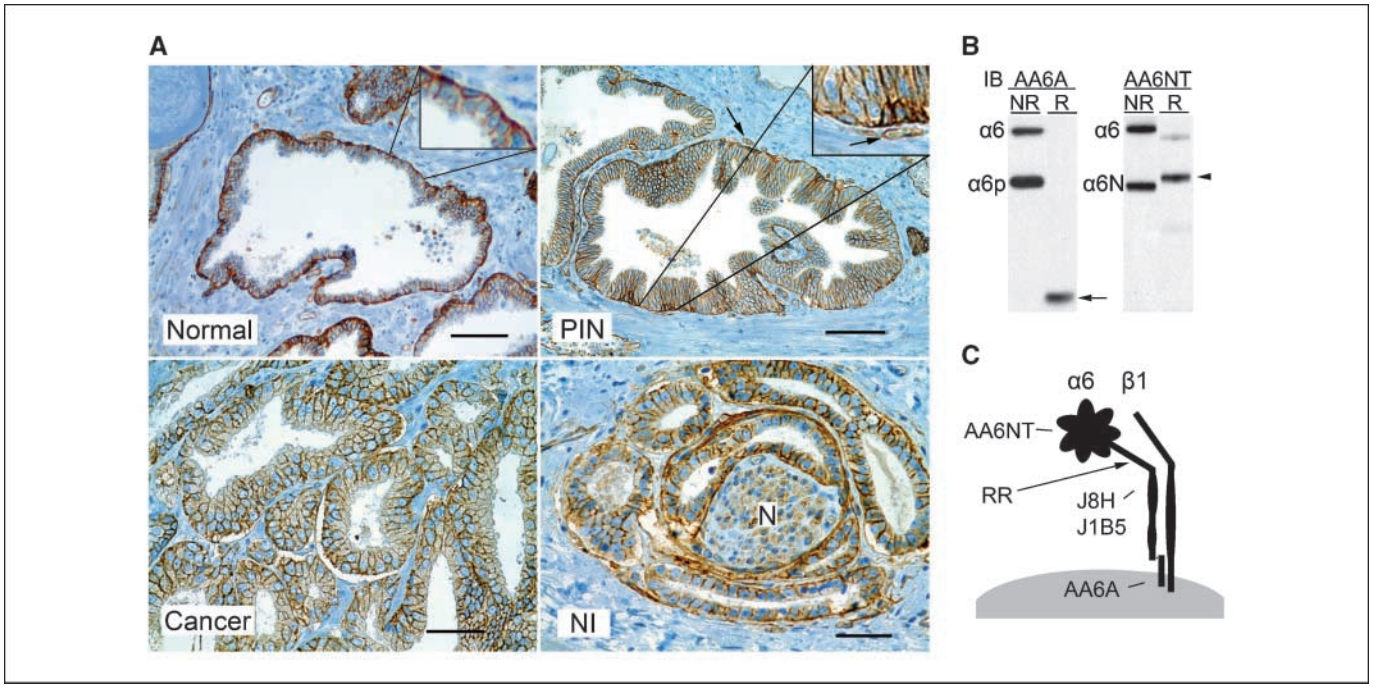

Figure 1. Integrin α_6 expression in human prostate cancer progression and antibody specificity. *A,* normal glands (*Normal*), PIN, Gleason grade 3 + 3 invasive carcinoma (*Cancer*), and perineural and endoneural invasion (*NI*). Formalin-fixed, paraffin-embedded tissue was reacted with primary antibody (AA6NT). *Arrows,* vessels detected by AA6NT. *Black bar,* 80 μm (*top two panels*) and 40 μm (*bottom two panels*). *B,* immunoblot (*IB*) analysis of α_6 integrin retrieved from DU145 cell lysate by immunoprecipitation with anti-α_6 integrin antibody (J1B5). AA6A polyclonal antibody detects both full-length α_6 and α_6p forms under nonreducing (*NR*) conditions and the 25 kDa light chain (*arrow*) under reducing (*R*) conditions. AA6NT detects full-length integrin under NR conditions and the NH_2-terminal cleavage product α_6N (*arrowhead*) under NR and R conditions. *C,* schematic of the relative location of α_6 integrin epitopes and cleavage site (RR).

Dr. A. Sonnenberg (27). The integrin α_6 rat monoclonal antibody J1B5 was generated by Dr. Caroline H. Damsky (29). AA6NT, a rabbit polyclonal antibody, was generated against a recombinant fragment of the NH_2-terminal integrin α_6 β-barrel domain and was used for immunohistochemistry analysis of archival material. In contrast, AA6A is a rabbit polyclonal antibody, recognizing the intracellular COOH-terminal domain of α_6 integrin, previously characterized by us and used for Western blot analysis (21). Donkey anti-mouse Alexa 488-conjugated antibodies and anti-rabbit horseradish peroxidase antibodies were obtained from Invitrogen. Human, single-chain, activated, urokinase was obtained from Millipore. Growth factor-reduced Matrigel was from BD Biosciences.

Cell culture. Cells were maintained in Iscove's modified Dulbecco's medium (IMDM; Life Technologies) supplemented with 10% heat-inactivated fetal bovine serum (Hyclone Laboratories) and 1% penicillin/streptomycin (Invitrogen) at 37°C in a 5% CO_2 atmosphere at constant humidity. PC3 and DU145 cells were obtained from the American Type Culture Collection and PC3N cells were previously characterized by us (30). Cell line identities were verified using genomic probes reported by others (31). The PC3B1 cells were isolated from the bone marrow of severe combined immunodeficient (SCID) mice that had been injected 6 weeks previously with the PC3 cell line. The bone marrow containing the tumor cells was retrieved with PBS and the PC3B1 cells were propagated in tissue culture. PC3B1 α_6 wild-type (WT) and PC3B1 α_6 RR cell lines were grown under blasticidin (Invitrogen) selection pressure (3 μg/mL). 293FT cells, used for generation of lentivirus, were grown in MEM supplemented with 10% fetal bovine serum and geneticin (500 μg/mL; Invitrogen). For antibody blocking experiments, cells were grown under optimal growth conditions for 24 h followed by replacement of medium with 5 mL complete IMDM containing J8H (20 μL/mL). J8H/medium replacement was done every 24 h.

Human prostate tissue immunohistochemistry. Prostate tissues were harvested, fixed in 10% neutral buffered formalin for 24 h, processed, and embedded in paraffin using the Tissue Acquisition and Cellular/Molecular Analysis Shared Service of The Arizona Cancer Center. Immunohistochemistry was done using the affinity-purified AA6NT rabbit polyclonal antibody diluted to 1:700 and stained on a Discovery XT Automated Immunostainer (Ventana Medical Systems). Antigen retrieval was done using a borate-EDTA at 100°C.

uPA-mediated cleavage of α_6 integrin. In immunoprecipitation experiments (21), α_6 integrin was retrieved from PC3N lysate using antibodies J1B5 or J8H for 3 h at 4°C and the resulting Sepharose G beads were resuspended in 500 μL Dulbecco's PBS (Invitrogen) with 20 ng activated single-chain uPA. The mixture was incubated overnight at 4°C with rotation, centrifuged, resuspended in nonreducing gel sample buffer, and analyzed by SDS-PAGE. In cell surface experiments, PC3N cells were harvested with PBS containing 5 mmol/L EDTA and resuspended in 500 μL serum-free IMDM. Cells were incubated for 30 min with or without J8H antibody at 4°C. Activated uPA (25 μg) was added to the cells and incubated for 3 h at 37°C. Cells (5×10^6) were washed once in PBS and lysed in radioimmunoprecipitation assay buffer (50 mmol/L Tris, 150 nmol/L NaCl, 1% Triton, 0.10% SDS, 1% deoxycholate, 1 mmol/L phenylmethylsulfonyl fluoride, 1 mmol/L leupeptin, and 1 mmol/L aprotinin). Following immunoprecipitation, samples were analyzed by SDS-PAGE.

Flow cytometry. Cells were harvested using PBS containing 5 mmol/L EDTA, washed in PBS, and resuspended in 200 μL PBS with 0.02% bovine serum albumin with J8H hybridoma supernatant (1:20). All antibody incubations were carried out on ice for 30 min. Antibody binding was detected by Alexa 488 anti-mouse secondary antibody (1:1,000) and analyzed using the Flow Cytometry Service of The Arizona Cancer Center.

Invasion assay. Growth factor-reduced Matrigel (50 μL) diluted (1:3) with serum-free IMDM was placed in 8.0 μm cell culture inserts (BD Falcon) and allowed to solidify for 1 h at 37°C. Inserts were placed into a 24-well plate. PC3B1 cells (1×10^5) were placed in the top insert chamber with 200 μL serum-free IMDM. IMDM (600 μL) supplemented with 10% fetal bovine serum was pipetted into the bottom well below the insert. After a 20 h incubation, inserts were washed in PBS and Matrigel was removed with a cotton swab. Cells on the underside of the insert were fixed/permeabilized in methanol/acetone and stained with 4′,6-diamidino-2-phenylindole (1 μg/mL) for nuclei detection. Cell numbers were counted using a

Published OnlineFirst June 2, 2009; DOI: 10.1158/0008-5472.CAN-09-0354

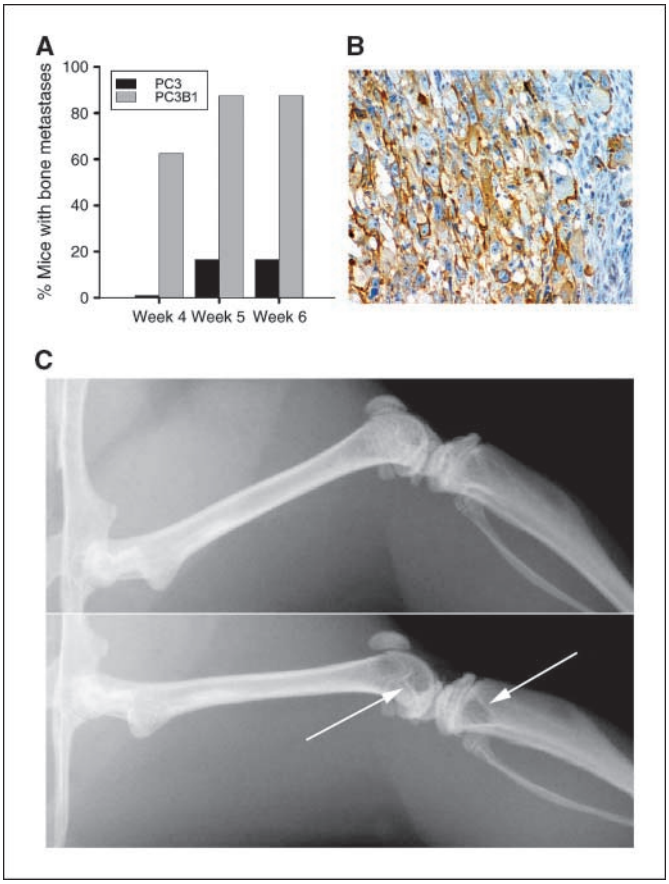

Figure 2. Characterization of a SCID mouse model of extravasation and bone metastasis. *A,* comparison of extravasation ability of PC3 and PC3B1 cells. *B,* immunohistochemistry analysis of α_6 integrin expression on PC3 cells within the mouse trabecular bone using AA6NT antibody. *C,* representative digital radiographs of mouse bone. *Top,* normal bone; *bottom,* presence of osteolytic metastases in the distal femur and proximal tibia (*arrows*) at week 4.

Zeiss Axiophot inverted microscope. Three images were collected per insert and experiments were done in triplicate.

SCID mouse model of extravasation. Mice experiments were conducted with animal care and use committee approval and done using the facilities and staff of the Experimental Mouse Shared Service at The Arizona Cancer Center. Left ventricle injections of single-cell suspensions of ~0.5 million cells in 0.2 mL PBS were done with a 27-gauge needle as described previously (32, 33). Mice were anesthetized with isoflurane (2-3% delivered through a nose cone). Twelve mice were used in each treatment group as dictated by statistical power analysis software.[5] One-way ANOVA between two treatment groups was used as the model with a 80% chance of detecting a difference and no more than a 5% chance of error. Mice receiving incorrectly placed injections or containing chest tumors at necropsy were removed from the study. Animals were terminated by CO_2 inhalation if microfractures were detected by radiographic images or if they showed signs of pain/suffering as specified by protocol.

Radiographic imaging. Animals were anesthetized with intraperitoneal injections of ketamine/HCl (50 mg/kg) and xylazine (15-20 mg/kg). Digital radiographs were collected on live animals 4, 5, and 6 weeks after tumor cell injection using a Faxitron MX-20 machine at 7 μm nominal resolution with a X-ray current of 300 μA and a voltage of 26 kV (Faxitron X-ray). Each digital image required 10 s. Animals were allowed to recover from anesthesia and returned to the animal care facility. Images were read and interpreted by G.D.P. (board-certified radiologist) without knowledge of the treatment groups.

Generation of PC3B1 integrin α_6 RR and WT mutant cell lines. The α_6 integrin cDNA was amplified with primers (5′-CACCCGACTCACTATAGGGAGACCCAAGC and 3′-CTATGCATCAGAAGTAAGCCTCTCTTTATCAGATG) and directionally cloned into the pENTR/D-TOPO vector (Invitrogen). The QuikChange II XL site-directed mutagenesis kit (Stratagene) was used to introduce alanine mutations at arginine residues 594 and 595 (RR), with primers previously characterized (21). Using the Gateway recombination cloning method (ref. 34; Invitrogen), α_6 integrin WT and RR mutant pENTR/D-TOPO vectors were recombined into the pLenti/UbC/V5-DEST expression vector. Generation of replication-incompetent lentiviral stocks was done by transfecting the pLenti/UbC/α_6 integrin vector in combination with ViraPower Packing Mix and Lipofectamine 2000 (Invitrogen) into 293FT cells. Virus was harvested after 72 h, centrifuged at high speed for 20 min at 4°C, and frozen at −80°C. Lentivirus was used to infect PC3B1 cells. Three days following transfection, cells were placed under blasticidin (3 μg/mL) selection. Expression of UbC-driven α_6 integrin RR mutant expression was confirmed by reverse transcription-PCR as described previously (28).

Results

Expression of α_6 integrin on tumor cell surface during escape from human prostate gland. Previous work has shown α_6 integrin expression in human normal prostate, prostatic intraepithelial neoplasia (PIN), and invasive cancer using frozen tissues and indirect immunofluorescence microscopy. Here, using an alternative method with human formalin-fixed, paraffin-embedded archival prostate tissue, we show simultaneous detection of tumor cell antigens and cell types (fibroblast, Schwann, and endothelial) or structures (nerves and vessels). Detection of α_6 integrin using formalin-fixed, paraffin-embedded tissues confirmed that normal prostate epithelial cells display polarized expression of α_6 integrin

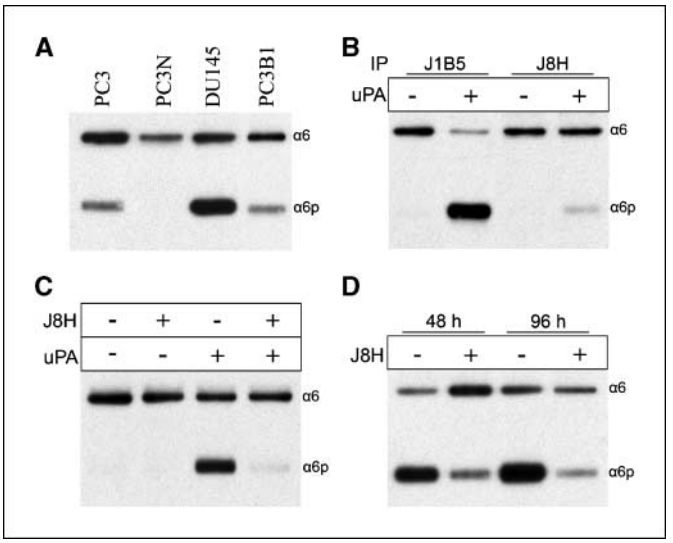

Figure 3. J8H engagement of α_6 integrin blocked uPA-mediated cleavage. In all panels, α_6 integrin was retrieved from cell lysates by immunoprecipitation (*IP*) with anti-α_6 integrin antibody followed by immunoblot detection of full-length α_6 (α_6) or cleaved α_6 (α_6p) using AA6A antibody. *A,* immunoblotting analysis of constitutive levels of α_6 and α_6p from prostate cancer cell lines. *B,* immunoprecipitation of α_6 integrin from PC3N lysate using J1B5 or J8H antibodies and treatment of the immunoprecipitation with activated uPA (20 ng/500 μL) for 18 h. *C,* PC3N cells were pretreated with or without the antibody J8H before being incubated with uPA (25 μg/500 μL) for a period of 3 h. *D,* DU145 cells received daily treatments of J8H for periods up to 96 h.

[5] http://www.cs.uiowa.edu/~rlenth/Power/

Published OnlineFirst June 2, 2009; DOI: 10.1158/0008-5472.CAN-09-0354

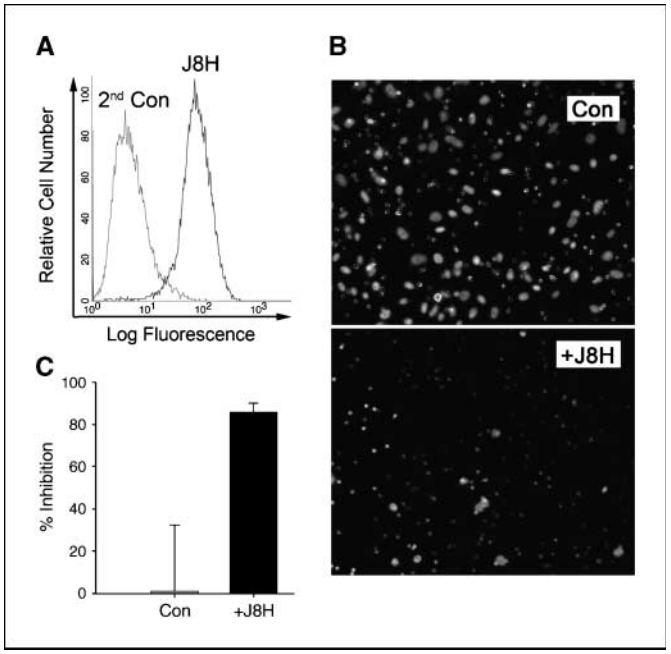

Figure 4. J8H inhibited the invasive potential of PC3B1 cells through Matrigel. *A,* flow cytometric analysis of α_6 integrin surface expression on PC3B1 using J8H antibody. *B,* Matrigel invasion assay detected cells that invaded to the underside of the insert by 4′,6-diamidino-2-phenylindole staining. *Top,* untreated PC3B1 cells (*Con*); *bottom,* PC3B1 cells in the presence of J8H antibody (+ *J8H*; 1 mg/mL). *C,* inhibition of invasion by J8H antibody. Mean ± SE of three independent experiments. Percent inhibition of J8H-treated cells was based on PC3B1 control untreated data.

at the basal cell/stromal interface (Fig. 1*A, Normal*) as shown previously by us and others (14).

We observed loss of α_6 integrin polarity during progression from PIN (Fig. 1*A, PIN*) to invasive cancer (Fig. 1*A, Cancer*). α_6 Integrin was expressed by vessels (Fig. 1*A, PIN, arrowhead*) as reported previously. We also show a new finding that α_6 integrin was expressed on the tumor cell surface during neural invasion (Fig. 1*A, NI*). Neural invasion by the tumor includes invasion both around and within the nerve. Perineural and endoneural invasion is characteristic of tumor present in the peripheral zone of the prostate gland (6, 35). The presence of α_6 integrin on perineural fibroblasts and Schwann cells of the nerve were observed, consistent with previous reports (36–38). Both antibodies (AA6A and AA6NT) used in this study recognize the full-length α_6 integrin by Western blot (Fig. 1*B*). The AA6A antibody was generated against the COOH-terminal cytoplasmic domain of the α_6 integrin and thus will recognize the cleaved integrin receptor α_6p under nonreduced conditions (NR). Under reducing conditions (R), AA6A recognizes the α_6 light chain that is shifted to ~25 kDa. In contrast, the AA6NT antibody, raised against the NH_2-terminal domain of the α_6 integrin, recognizes the NH_2-terminal fragment, called α_6N. The α_6N heavy chain shifts to an apparent larger MW on reduction (R), as expected. A schematic illustrating the relative location of the epitopes on integrin α_6 recognized by the four antibodies (AA6NT, J8H, J1B5, and AA6A) used in this study and the uPA cleavage site (RR) is shown (Fig. 1*C*).

SCID mouse model of prostate cancer extravasation. Injection of human tumor cells into the left ventricle of the mouse heart ensured broad dissemination of tumor cells via the circulation. The model is relevant to human prostate cancer progression because metastases develop from the arterial distribution of tumor emboli in circulation (39). We developed a model for generating reproducible and aggressive bone metastases by comparing the effectiveness of PC3 cells versus PC3B1 cells (Fig. 2*A*). Human tumor within the bone expressed α_6 integrin on the cell surface (Fig. 2*B*). Radiograph images of the entire skeleton were surveyed on all animals and a metastasis in any bone resulted in a positive score. All bone metastases detected were lytic lesions located primarily within the metaphysis and abutting the epiphyseal plate (Fig. 2*C, arrows*), and all were progressive (data not shown). This model system enabled testing of how tumor cell properties influence extravasation and development of bone metastases.

α_6 integrin antibody J8H inhibited uPA-mediated cleavage of α_6 integrin. Prostate cancer cell lines PC3, PC3N, DU145, and PC3B1 produced varying amounts of α_6p under normal growth conditions (Fig. 3*A*). The PC3N cell line was chosen for further study because α_6 integrin expressed on the cell surface was primarily in the full-length form. α_6 Integrin was retrieved via immunoprecipitation using either J1B5 or J8H antibody and its ability to be cleaved was tested by addition of uPA. α_6 integrin retrieved by J1B5 was converted to α_6p integrin in the presence of uPA

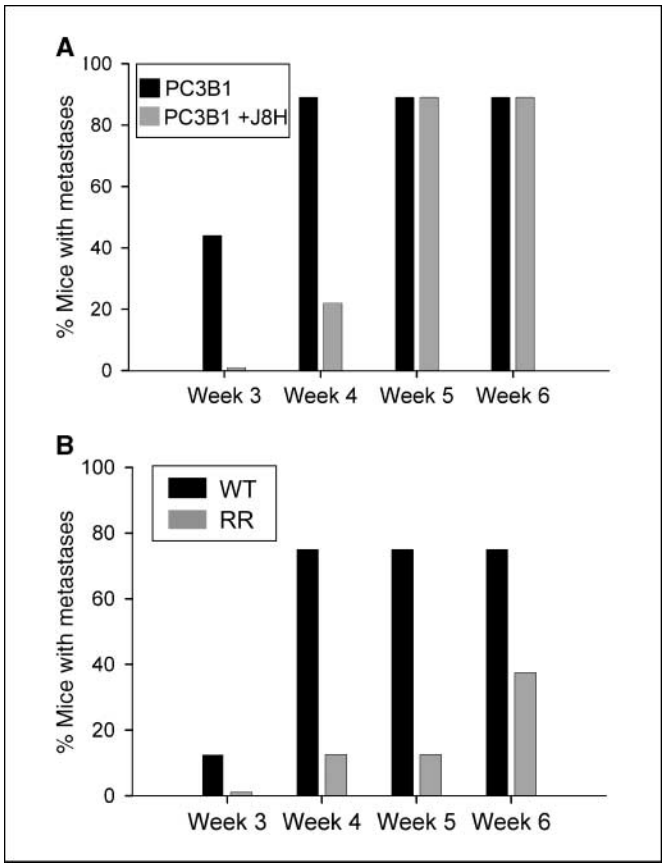

Figure 5. J8H antibody or genetic inhibition of α_6 integrin cleavage inhibited bone metastases. *A,* SCID mice were injected with untreated PC3B1 cells (PC3B1) or cells containing surface-bound J8H (PC3B1 + J8H). *B,* SCID mice were injected with PC3B1 cells expressing a cleavable α_6 integrin (WT) or an uncleavable α_6 integrin mutant (RR). In both panels, the entire skeleton of the mouse was inspected for metastases using digital radiographs collected at 3, 4, 5, and 6 wk after injection. The presence of an osteolytic lesion in any bone was scored as a positive metastasis and all metastatic lesions were progressive (data not shown). The analysis was done without knowledge of the treatment groups. Sample size contained 12 mice per treatment group.

Published OnlineFirst June 2, 2009; DOI: 10.1158/0008-5472.CAN-09-0354

Table 1. Radiographic detection of bone metastases

Mouse/PC3B1	Week 3	Week 4	Week 5	Week 6
1	Normal	RDF	RDF, LDF	Terminated
2	Normal	LDF, LPT	Terminated	Terminated
3	RPT	RDF, RPT, LPT	Terminated	Terminated
4	Normal	RF, LT, LF	Terminated	Terminated
5	Normal	Normal	Normal	Terminated
6	RDF	RDF, RPT	Terminated	Terminated
7	RPT	RPT, LPT	Terminated	Terminated
8	RPT	RPT	Terminated	Terminated
9	Normal	RPT	Terminated	Terminated
Mouse/PC3B1 +J8H				
10	Normal	Normal	RPT	Terminated
11	Normal	Normal	LPT, RPF	Terminated
12	Normal	LDF, LPT	RT, LDF, LPT	Terminated
13	Normal	LDF, LDT	LDF, LPT,	Terminated
14	Normal	Normal	Normal	Terminated
15	Normal	Normal	RDF, LDF, LPT	Terminated
16	Normal	Normal	RT, LT	Terminated
17	Normal	Normal	LDF	Terminated
18	Normal	Normal	PRF	Terminated
Mouse/PC3B1-WT				
1	Normal	Normal	Normal	Normal
2	Positive LDF	Progressive LDF	Progressive LDF	Progressive LDF
3	Normal	Positive RDF	Progressive RDF	Progressive RDF
4	Normal	Positive RDF	Progressive RDF	Progressive RDF
5	Normal	Normal	Normal	Normal
6	Normal	Positive RDF	Progressive RDF	Progressive RDF
7	Normal	Positive LDF	Progressive LDF	Progressive LDF
8	Normal	Positive LDF, R fibula thin	Progressive LDF, R fibula thinner	Progressive LDF, R fibula gone
Mouse/PC3B1-RR				
9	Normal	Normal	Normal	Normal
10	Normal	Positive RT	Progressive RT	Progressive RT
11	Normal	Normal	Normal	Normal
12	Normal	Normal	Normal	Normal
13	Normal	Normal	Normal	Positive RDF
14	Normal	Normal	Normal	Normal
15	Normal	Normal	Normal	Normal
16	Normal	Normal	Normal	Positive RDF

Abbreviations: Location of bone lesions: RDF, right distal femur; LDF, left distal femur; LPT, left proximal tibia; RPT, right proximal tibia; RF, right femur; LT, left tibia; RT, right tibia; LF, left femur; RPF, right proximal femur.

as shown by the decrease in the full-length form (α_6) and a corresponding increase in α_6p form (Fig. 3*B*). In contrast, α_6 integrin retrieved by J8H remained in the full-length form (α_6) in the presence of uPA (Fig. 3*B*).

We next tested if J8H antibody blocked integrin cleavage on the cell surface. PC3N cells were pretreated with or without J8H before incubation with uPA. In the absence of J8H and uPA or the absence of uPA alone, the α_6 integrin remained in the full-length form on the cells (Fig. 3*C*). The addition of uPA without the J8H antibody resulted in α_6 integrin converted to α_6p as shown by the decrease in the full-length form (α_6) and a corresponding increase in the cleavage product, α_6p (Fig. 3*C*). Importantly, pretreatment of cells with J8H antibody prevented the production of the cleaved form (α_6p) via uPA (Fig. 3*C*). These results indicated that induction of α_6p by the exogenous addition of uPA can be blocked by either engaging the α_6 integrin in an immunoprecipitation reaction or engaging α_6 integrin on the cell surface with the antibody, J8H.

We next tested if J8H could block the production of α_6p in DU145 cells. DU145 cells were selected for this experiment because they do not require exogenous addition of uPA to generate α_6p integrin (Fig. 3*A*). Previously published data indicated that the biological half-life of α_6p on the cell surface was ~72 h (40). Therefore, experiments were designed to test the ability of J8H to block endogenous α_6p production over several days. J8H treatment of DU145 cells for 48 h dramatically decreased the endogenous production of α_6p (Fig. 3*D*). Inhibition of α_6p production was also observed after 96 h.

J8H diminished the invasive potential of PC3B1 cells. The data thus far indicated that J8H prevented α_6p production. Previous work suggested that preventing α_6p production would decrease cell migration on laminin (21, 28). Because tumor

Published OnlineFirst June 2, 2009; DOI: 10.1158/0008-5472.CAN-09-0354

invasion of laminin-coated nerves was observed (Fig. 1*A*), we next determined whether J8H altered cancer cell invasion on laminin. We used a Matrigel invasion assay in the presence of purified laminin 111, a ligand of α_6 integrin. PC3B1 cells were selected for this experiment due to their aggressive nature in the mouse metastasis model and because they produce α_6p (Fig. 2*A*). We first confirmed, through flow cytometry, that PC3B1 cells have surface expressed α_6 integrin recognized by the J8H antibody (Fig. 4*A*). Cells were applied to Matrigel-coated inserts in the presence of J8H to determine if invasion was altered. After 20 h of incubation, the ability of PC3B1 cells to invade (control) was inhibited significantly in the presence of J8H antibody (Fig. 4*B*). The image results were quantitated and ~80% of the cells were inhibited from reaching the underside of the Matrigel-coated insert in the presence of J8H (Fig. 4*C*).

Pretreatment of PC3B1 cells with J8H significantly delayed bone metastasis. Using the SCID mouse model of extravasation, we tested whether engagement of the α_6 integrin with J8H, the cleavage blocking antibody, would inhibit bone metastasis. Previous work by others showed that tumor cells within the circulation can extravasate to bone within 1 to 2 h of injection (41–43). Titration analysis of the J8H antibody was done by flow cytometry on PC3B1 cells to determine maximal surface labeling (data not shown). PC3B1 cells alone or J8H-treated cells were introduced into the circulation of SCID mice. The percentage of mice containing bone metastases was determined by digital radiographs of live animals 3, 4, 5, and 6 weeks later (Fig. 5*A*). Injection of PC3B1 cells resulted in ~40% of the animals containing bone metastases within 3 weeks, and by 4 weeks, 80% of the animals contained bone metastasis (Fig. 5*A*). By week 5, 80% of the animals required termination (Table 1). In contrast, injection of PC3B1 cells pretreated with J8H resulted in no metastases within 3 weeks, and at 4 weeks, 80% of the animals were free of bone metastasis (Fig. 5*A*). Interestingly, by week 5, 80% of the animals displayed bone metastases. By week 6, 80% of the animals required termination (Table 1). The lesions detected in both groups of animals were osteolytic and progressive and arose primarily within the distal femur or proximal tibia (Table 1). Of particular note, no lesions were detected in the vertebral column, the pelvic girdle, mandible, or skull (data not shown).

Mutation of α_6 integrin cleavage site prevented PC3B1 bone metastasis. Our next step was to validate the J8H blocking results and determine if expression of an uncleavable α_6 integrin in tumor cells would prevent extravasation to bone. We expressed the mutant form of α_6 integrin, called RR, in PC3B1 cells. Endogenous levels of α_6 integrin were not altered in this experiment. We have shown previously that cellular expression of the integrin RR mutant results in a fully functional receptor expressed on the cell surface, laminin-dependent adhesion, and viable tumor xenografts in a mouse model (21, 28). PC3B1 cells were transfected with either WT α_6 integrin (PC3B1-WT) or α_6 integrin containing alanine substitutions for arginine at amino acid positions 594 and 595 (PC3B1-RR). The expression level of the α_6 integrin on the cell surface was comparable between the groups as determined by fluorescence-activated cell sorting analysis (data not shown). Injection of PC3B1-WT cells resulted in detectable bone metastasis in ~10% of the animals within 3 weeks and 80% of the animals by weeks 4, 5, and 6 (Fig. 5*B*, *WT*). In contrast, injection of the PC3B1-RR cells resulted in no lesions within 3 weeks, and only 10% of the animals showed lesions by weeks 4 and 5 (Fig. 5*B*, *RR*). By week 6, less than half of the animals had detectable metastatic lesions (Table 1). Radiographically, lesions that developed in the PC3B1-RR group were sharply circumscribed and not strikingly expansile compared with the PC3B1-WT. Of particular note, no lesions were detected in the vertebral column, the pelvic girdle, mandible, or skull (data not shown). Necropsy analysis detected no lesions in the lung, liver, or adrenal gland (data not shown).

Discussion

In this study, we show that inhibiting α_6 integrin cleavage on the tumor cell surface, either through antibody engagement or integrin mutation, will substantially delay the appearance of osseous metastases in a mouse xenograft model. The results reported here support the hypothesis that α_6 integrin cleavage permits extravasation of tumor cells from the circulation because subcutaneous injection or direct injection of PC3N-RR mutant cells into bone has no affect on tumor growth at either location (28, 44). This is significant in the course of the human disease because extravasation from the circulation is a critical factor of metastatic spread (8, 39).

The influence of antibody engagement to delay the metastatic phenotype suggests that providing circulating levels of the integrin-specific antibody may be beneficial in preventing bone metastasis. The ability of J8H to reversibly delay the appearance of metastases by 1 week is significant because this corresponds to the expected half-life of therapeutic-type antibodies in the SCID mouse (45). Toxicity of J8H in the normal tissue is not expected because this antibody does not block cell adhesion to laminin (27). Previous work has shown that inhibiting the α_6 adhesion function will block experimental metastasis to the lung (14). However, the utility of this approach as a therapeutic strategy appears limited. Circulating levels of immunoglobulin specific for blocking α_6 integrin adhesion function in humans result in the formation of blisters and erosive lesions in the oral mucosa (25, 26). This underscores the potential therapeutic benefits of the J8H antibody, a reagent that inhibits α_6 cleavage and not α_6-dependent adhesion.

α_6 integrin is used by hematopoietic stem cells to target the bone (46). The ability of the α_6 integrin RR mutation to reduce the metastatic potential of tumor cells homing to bone occurs in the presence of endogenous WT α_6 integrin. This leads to speculation that cleavage of the receptor has a dominant role in the process. The results indicate that both the time to metastasis and the number of mice developing bone lesions were substantially reduced in the PC3B1-RR group. In contrast to the antibody blocking experiments, the majority of the animals did not develop bone lesions over the 6-week course of the study. Necropsies of the animals receiving tumor cell injections did not reveal other common sites of metastasis (lung, liver, or adrenal gland), suggesting that circulating tumor cells were either eliminated from the mouse or achieved a level of dormancy (47, 48) in the animal. Further experiments using labeled cells and sensitive imaging technology as developed by other groups (49) could distinguish these possibilities.

It is also interesting to note that, after week 6, ~40% of the animals injected with PC3B1-RR mutant cells developed a detectable metastatic lesion in bone. Although these lesions were progressive, the rate of progression compared with PC3B1-WT was slow as determined by the radiographic features of observed lesions. Termination of these animals was not required because metastases did

Published OnlineFirst June 2, 2009; DOI: 10.1158/0008-5472.CAN-09-0354

not produce aggressive lesions leading to pathologic fractures. This suggests that tumor cells that possess uncleavable α_6 integrin may eventually adapt to and colonize an osseous microenvironment to produce lytic lesions but remain less aggressive in nature. This result is consistent with the reported less aggressive phenotype of the RR mutant tumor cells directly injected into the distal end of a mouse femur (28).

We note that endogenous levels of α_6p observed for cell lines in culture do not correlate with secreted levels of uPA and uPA activity. PC3 cells express minimal levels of α_6p, whereas DU145 cells convert a majority of α_6 integrin into the cleaved product (Fig. 3*A*). However, PC3 cells secrete at least 2-fold more active uPA when compared with DU145 (50). This suggests that uPA concentration is not the limiting factor in the regulation of integrin α_6 cleavage. The ability to block α_6 integrin cleavage by extracellular engagement of the receptor points to the possibility that lateral membrane associations with surface-expressed proteins, such as tetraspanins (51, 52) and uPA receptor (uPAR; refs. 53, 54), could influence uPA-mediated integrin cleavage in a physiologically relevant manner. Current work investigating this possibility may reveal other potential cell surface targets for disruption of extravasation of prostate cancer to bone.

The amount of α_6p *in vitro* is not prognostic for bone metastasis *in vivo*. However, the inability to produce α_6p will significantly hinder bone metastasis development in mice. It will be important to have a method to detect cleaved α_6p *in vivo* to determine if the cleaved integrin could serve as a prognostic factor. We are currently developing an ELISA to determine if the released extracellular fragment of α_6 integrin is detectable in blood. We consider it likely that α_6 cleavage may add to the multiple molecular features required to reliably detect tumor cells with metastatic potential.

Disclosure of Potential Conflicts of Interest

No potential conflicts of interest were disclosed.

Acknowledgments

Received 2/2/09; revised 3/23/09; accepted 4/22/09; published OnlineFirst 6/2/09.

Grant support: NIH grants T32CA009213, P30 CA23074, and PO1 CA56666.

The costs of publication of this article were defrayed in part by the payment of page charges. This article must therefore be hereby marked *advertisement* in accordance with 18 U.S.C. Section 1734 solely to indicate this fact.

We thank the dedicated staff of the Tissue Acquisition Core Service, the Experimental Mouse Shared Service, and the Flow Cytometry Service located in The Arizona Cancer Center.

References

1. Hangan D, Morris VL, Boeters L, von Ballestrem C, Uniyal S, Chan BM. An epitope on VLA-6 ($\alpha_6\beta_1$) integrin involved in migration but not adhesion is required for extravasation of murine melanoma B16F1 cells in liver. Cancer Res 1997;57:3812–7.
2. Friedrichs K, Ruiz P, Franke F, Gille I, Terpe HJ, Imhof BA. High expression level of α_6 integrin in human breast carcinoma is correlated with reduced survival. Cancer Res 1995;55:901–6.
3. Tagliabue E, Ghirelli C, Squicciarini P, Aiello P, Colnaghi MI, Menard S. Prognostic value of $\alpha_6\beta_4$ integrin expression in breast carcinomas is affected by laminin production from tumor cells. Clin Cancer Res 1998;4:407–10.
4. Danen EH, van Muijen GN, van de Wiel-van Kemenade E, Jansen KF, Ruiter DJ, Figdor CG. Regulation of integrin-mediated adhesion to laminin and collagen in human melanocytes and in non-metastatic and highly metastatic human melanoma cells. Int J Cancer 1993; 54:315–21.
5. van der Flier A, Sonnenberg A. Function and interactions of integrins. Cell Tissue Res 2001;305:285–98.
6. Ayala GE, Dai H, Powell M, et al. Cancer-related axonogenesis and neurogenesis in prostate cancer. Clin Cancer Res 2008;14:7593–603.
7. Villers A, McNeal JE, Redwine EA, Freiha FS, Stamey TA. The role of perineural space invasion in the local spread of prostatic adenocarcinoma. J Urol 1989;142: 763–8.
8. Jacobs SC. Spread of prostatic cancer to bone. Urology 1983;21:337–44.
9. Singh G, Orr FW. Bone metastasis and molecular mechanisms: pathophysiology. Dordrecht: Kluwer Academic; 2004; xvi, 308.
10. Siler U, Seiffert M, Puch S, et al. Characterization and functional analysis of laminin isoforms in human bone marrow. Blood 2000;96:4194–203.
11. Gu Y, Sorokin L, Durbeej M, Hjalt T, Jonsson JI, Ekblom M. Characterization of bone marrow laminins and identification of α_5-containing laminins as adhesive proteins for multipotent hematopoietic FDCP-Mix cells. Blood 1999;93:2533–42.
12. Gu YC, Kortesmaa J, Tryggvason K, et al. Laminin isoform-specific promotion of adhesion and migration of human bone marrow progenitor cells. Blood 2003; 101:877–85.
13. Fornaro M, Manes T, Languino LR. Integrins and prostate cancer metastases. Cancer Metastasis Rev 2001;20:321–31.
14. Cress AE, Rabinovitz I, Zhu W, Nagle RB. The $\alpha_6\beta_1$ and $\alpha_6\beta_4$ integrins in human prostate cancer progression. Cancer Metastasis Rev 1995;14:219–28.
15. Nagle RB, Hao J, Knox JD, Dalkin BL, Clark V, Cress AE. Expression of hemidesmosomal and extracellular matrix proteins by normal and malignant human prostate tissue. Am J Pathol 1995;146:1498–507.
16. Hao J, Yang Y, McDaniel KM, Dalkin BL, Cress AE, Nagle RB. Differential expression of laminin 5 ($\alpha_3\beta_3\gamma_2$) by human malignant and normal prostate. Am J Pathol 1996;149:1341–9.
17. Demetriou MC, Cress AE. Integrin clipping: a novel adhesion switch? J Cell Biochem 2004;91:26–35.
18. Demetriou MC, Pennington ME, Nagle RB, Cress AE. Extracellular α_6 integrin cleavage by urokinase-type plasminogen activator in human prostate cancer. Exp Cell Res 2004;294:550–8.
19. Sheng S. The urokinase-type plasminogen activator system in prostate cancer metastasis. Cancer Metastasis Rev 2001;20:287–96.
20. Shariat SF, Roehrborn CG, McConnell JD, et al. Association of the circulating levels of the urokinase system of plasminogen activation with the presence of prostate cancer and invasion, progression, and metastasis. J Clin Oncol 2007;25:349–55.
21. Pawar SC, Demetriou MC, Nagle RB, Bowden GT, Cress AE. Integrin α_6 cleavage: a novel modification to modulate cell migration. Exp Cell Res 2007;313:1080–9.
22. Ginsberg MH, Partridge A, Shattil SJ. Integrin regulation. Curr Opin Cell Biol 2005;17:509–16.
23. Hynes RO. Integrins: bidirectional, allosteric signaling machines. Cell 2002;110:673–87.
24. Tsuchida J, Ueki S, Saito Y, Takagi J. Classification of 'activation' antibodies against integrin β_1 chain. FEBS Lett 1997;416:212–6.
25. Rashid KA, Stern JN, Ahmed AR. Identification of an epitope within human integrin α_6 subunit for the binding of autoantibody and its role in basement membrane separation in oral pemphigoid. J Immunol 2006;176: 1968–77.
26. Mignogna M, Lanza A, Rossiello L, Ruocco V, Ahmed AR. Comparison of reactivity and epitope recognition between sera from American and Italian patients with oral pemphigoid. Clin Exp Immunol 2006;145:28–35.
27. Hogervorst F, Kuikman I, Noteboom E, Sonnenberg A. The role of phosphorylation in activation of the $\alpha_{6A}\beta_1$ laminin receptor. J Biol Chem 1993;268:18427–30.
28. King TE, Pawar SC, Majuta L, et al. The role of α_6 integrin in prostate cancer migration and bone pain in a novel xenograft model. PLoS ONE 2008;3:3535.
29. Damsky CH, Librach C, Lim KH, et al. Integrin switching regulates normal trophoblast invasion. Development 1994;120:3657–66.
30. Tran NL, Nagle RB, Cress AE, Heimark RL. N-cadherin expression in human prostate carcinoma cell lines. An epithelial-mesenchymal transformation mediating adhesion with stromal cells. Am J Pathol 1999; 155:787–98.
31. van Bokhoven A, Varella-Garcia M, Korch C, Hessels D, Miller GJ. Widely used prostate carcinoma cell lines share common origins. Prostate 2001;47:36–51.
32. Arguello F, Baggs RB, Frantz CN. A murine model of experimental metastasis to bone and bone marrow. Cancer Res 1988;48:6876–81.
33. Arguello F, Furlanetto RW, Baggs RB, et al. Incidence and distribution of experimental metastases in mutant mice with defective organ microenvironments (genotypes Sl/Sld and W/Wv). Cancer Res 1992;52:2304–9.
34. Ohara O, Temple G. Directional cDNA library construction assisted by the *in vitro* recombination reaction. Nucleic Acids Res 2001;29:22.
35. Lee SB, Hong SK, Choe G, Lee SE. Periprostatic distribution of nerves in specimens from non-nerve-sparing radical retropubic prostatectomy. Urology 2008;72:878–81.
36. Niessen CM, Cremona O, Daams H, Ferraresi S, Sonnenberg A, Marchisio PC. Expression of the integrin $\alpha_6\beta_4$ in peripheral nerves: localization in Schwann and perineural cells and different variants of the β_4 subunit. J Cell Sci 1994;107:543–52.
37. Sonnenberg A, Linders CJ, Daams JH, Kennel SJ. The $\alpha_6\beta_1$ (VLA-6) and $\alpha_6\beta_4$ protein complexes: tissue distribution and biochemical properties. J Cell Sci 1990;96:207–17.
38. Nodari A, Zambroni D, Quattrini A, et al. β_1 Integrin activates Rac1 in Schwann cells to generate radial lamellae during axonal sorting and myelination. J Cell Biol 2007;177:1063–75.
39. Coman DR, deLong RP, McCutcheon M. Studies

Published OnlineFirst June 2, 2009; DOI: 10.1158/0008-5472.CAN-09-0354

on the mechanisms of metastasis; the distribution of tumors in various organs in relation to the distribution of arterial emboli. Cancer Res 1951;11:648–51.

40. Davis TL, Rabinovitz I, Futscher BW, et al. Identification of a novel structural variant of the α_6 integrin. J Biol Chem 2001;276:26099–106.

41. Harms JF, Welch DR. MDA-MB-435 human breast carcinoma metastasis to bone. Clin Exp Metastasis 2003;20:327–34.

42. Phadke PA, Mercer RR, Harms JF, et al. Kinetics of metastatic breast cancer cell trafficking in bone. Clin Cancer Res 2006;12:1431–40.

43. Wetterwald A, van der Pluijm G, Que I, et al. Optical imaging of cancer metastasis to bone marrow: a mouse model of minimal residual disease. Am J Pathol 2002;160:1143–53.

44. Pawar SC, Dougherty S, Pennington ME, et al. α_6 Integrin cleavage: sensitizing human prostate cancer to ionizing radiation. Int J Radiat Biol 2007;83:761–7.

45. Kaufmann R, Hainzl A, Sterry W, Alberti S, Klein CE. *In vivo* targeting of integrin receptors in human skin xenografts by intravenously applied antibodies. Arch Dermatol Res 1994;286:6–11.

46. Qian H, Georges-Labouesse E, Nystrom A, et al. Distinct roles of integrins α_6 and α_4 in homing of fetal liver hematopoietic stem and progenitor cells. Blood 2007;110:2399–407.

47. Wikman H, Vessella R, Pantel K. Cancer micrometastasis and tumour dormancy. APMIS 2008;116:754–70.

48. Allan AL, Vantyghem SA, Tuck AB, Chambers AF. Tumor dormancy and cancer stem cells: implications for the biology and treatment of breast cancer metastasis. Breast Dis 2006;26:87–98.

49. Kaijzel EL, Snoeks TJ, Buijs JT, van der Pluijm G, Lowik CW. Multimodal imaging and treatment of bone metastasis. Clin Exp Metastasis 2009;26:371–9.

50. Dondi D, Festuccia C, Piccolella M, Bologna M, Motta M. GnRH agonists and antagonists decrease the metastatic progression of human prostate cancer cell lines by inhibiting the plasminogen activator system. Oncol Rep 2006;15:393–400.

51. Hemler ME. Tetraspanin functions and associated microdomains. Nat Rev Mol Cell Biol 2005;6:801–11.

52. Berditchevski F. Complexes of tetraspanins with integrins: more than meets the eye. J Cell Sci 2001;114:4143–51.

53. Kugler MC, Wei Y, Chapman HA. Urokinase receptor and integrin interactions. Curr Pharm Des 2003;9:1565–74.

54. Tarui T, Mazar AP, Cines DB, Takada Y. Urokinase-type plasminogen activator receptor (CD87) is a ligand for integrins and mediates cell-cell interaction. J Biol Chem 2001;276:3983–90.